Optimization of MoO_3/Ag/MoO_3 Multilayer Transparent Conductive Electrodes via Thermal Annealing for Optoelectronics Application

Z. Nouri, F. Hajakbari*, A. Hojabri

Department of Physics, Ka. C., Islamic Azad University, Karaj, Iran.
Received: 16 May 2025 - Accepted: 20 October 2025

Abstract

Transparent conductive electrodes (TCEs) are an indispensable component in optoelectronic devices and organic solar cells (OSCs). Recently, oxide/metal/oxide multilayers have been identified as promising structures (TCEs). In this context, we prepared MoO_3/Ag/MoO_3 (MAM) multilayer structures on glass substrates at different Ag thicknesses using RF and DC magnetron sputtering. Samples were prepared with Ag thicknesses ranging from 5 to 10 nm. As a result of varying the Ag midlayer thickness, the MA (10nm) M trilayer structure with more desirable electrical, optical, and morphological properties compared to other samples was selected and was exposed to thermal annealing with an oxygen to argon flow ratio of 20% at temperatures of 400 and 500 °C for 2 h in an electric furnace. Investigations highlighted the prominent role of reactive thermal annealing in optimizing the properties of multilayer structures, which has led to improved stoichiometry of the MoO_3 layer and increased optical transmittance and electrical conductivity of trilayer structures. The MA(10 nm, 400 °C) M multilayers with a modified figure of merit of 23.86×10^{-3} (Ω^{-1}) as the optimal structure have potential application as TCEs in optoelectronic devices and (OSCs).

Keywords: Transparent Electrodes, Trilayer, RF Sputtering, Thermal Annealing, MoO_3, Ag.

1. Introduction

Renewable energy sources are naturally produced at a higher rate than they are consumed, while fossil energy resources are limited. Therefore, studying the use of renewable energy sources seems to be essential to chart a sustainable future for growing societies. These energy sources are reliable and clean alternatives to fossil fuels by reducing greenhouse gas emissions and mitigating climate change. Meanwhile, solar cells and their components have attracted a lot of attention. Transparent conductive electrodes (TCEs) are essential components in many optoelectronic devices, including solar cells. They are materials that are transparent in the visible light range and are also capable of conducting electrical charge [1]. However, the use of common transparent conductive oxides has encountered limitations that necessitate the need for an alternative. Recently, among emerging technologies, oxide/metal/oxide structures, in which a thin metal layer is sandwiches between two oxide layers, have been widely studied as promising electrodes [2-5]. Desired optical transmittance and electrical conductivity, flexibility, easy production and deposition capability on various substrates are among the numerous advantages of these structures [6]. The conductivity in these structures is through the metal layer [7], so a metal layer with high conductivity is required in such structures. In this regard, silver with the lowest resistivity, seems to be a suitable choice for the metal layer [8].

*Corresponding author
Email address: fatemeh.hajakbari@kiau.ac.ir

The thickness of the metal layer must be sufficient to provide conductivity of the structure [9].
The placement of oxide layers on the sides of the metal layer, leads to suppression of light reflection by the metal layer and leads to high transparency of the structure [7,10,11]. Molybdenum trioxide is a transition metal oxide and a n type semiconductor compound with a direct band gap and high work function that is relatively chemically stable.
This metal oxide is non-toxic and its abundance in nature is high [12], so it is a good choice as oxide layer in oxide/metal/oxide structures [13].
Therefore, MoO_3/Ag/MoO_3 multilayer structures can be used as TCEs [14]. To achieving desired performance in these structures, simultaneous attainment of high optical transmittance and electrical conductivity is required, which needs the study and use of appropriate laboratory methods and conditions. In this regard, in this study, we have prepared, optimized and characterized the MoO_3/Ag/MoO_3 multilayer structures and demonstrated their efficiency as TCEs. We prepared the MoO_3/Ag/MoO_3 structures using magnetron sputtering on glass substrates, then optimized the thickness of silver layer, and investigated the effect of thermal annealing in presence of oxygen gas and annealing temperature on the structural, morphological, electrical and optical properties of the prepared films.
Molybdenum trioxide-based trilayer were deposited on glass substrates sequentially using radio frequency magnetron sputtering of molybdenum trioxide target (99.99%) and direct current magnetron sputtering of Ag metal target (99.99%),

by varying the deposition time of the Ag layer in four separate steps without breaking the vacuum.

2 .Materials and Methods

All deposition steps were performed at constant sputtering power of 81 and 32 W for molybdenum trioxide and Ag layers respectively. Other deposition conditions including base pressure, working pressure and radio frequency sputtering time were kept constant at all four stages so that molybdenum trioxide layers were deposited symmetrically with a thickness of 60 nm on both sides of silver layers with thicknesses of 5,10,15 and 20 nm. The films thicknesses were monitored in situ. The substrates were fixed at a distance of 9 cm from the target. The deposition was applied at a working pressure of 8×10^{-3} mbar. After deposition, a number of samples were thermally annealed at temperatures of 400 and 500 ◦C for two hours in the presence of oxygen gas. The naming of multilayer structures deposited on glass substrates according to their Ag midlayer thickness and annealing temperature is shown in the Table 1. The structural properties of prepared samples were evaluated using an X-ray diffractometer (XRD; Philips PW3710) with Cukα radiation (λ= 0.1540nm). The surface morphology of multilayer structures was investigated using atomic force microscopy in noncontact mode (AFM; DS95-50 scanner, DME Company, Denmark). The elemental composition of prepared samples was determined using Energy-Dispersive X-ray Spectroscopy (EDX) analyzer which was attached to Field Emission Scanning Electron Microscopy (FESEM; Hitachi S-4160). A UV-VIS spectrometer was utilized to analyze the optical transmittance of samples (Perkin Elmer, Lambda25). The sheet resistance of multilayers was measured using four-point probe technique.

Table. 1. The naming of MoO_3/Ag/MoO_3 trilayer films.

Sample	Substrate	Ag Thickness (nm)	Annealing Temperature (◦C)
B_1	Glass	5	-
B_2	Glass	10	-
B_3	Glass	15	-
B_4	Glass	20	-
B_{23}	Glass	10	400
B_{24}	Glass	10	500

3. Results and Discussions

3.1. XRD analysis

The X-ray diffraction (XRD) patterns of the as deposited MAM multilayer structures with Ag thicknesses of 5, 10, 15 and 20 nm and MA(10nm)M annealed samples on glass substrates are shown in Fig. 1.(a) and Fig. 1.(b) respectively. In the XRD patterns of as deposited samples on glass substrates, no diffraction peak belonging to molybdenum trioxide or silver oxide is observed, indicating the amorphous nature of multilayer structures in these samples. The amorphous nature can be caused by the irregular arrangement of atoms, the presence of defects in the crystal, the lattice mismatch between the layer and the substrate, or the insufficient formation of particles on substrate [15-17]. Since the argon sputtering can create oxygen vacancy defects in metal oxide layers and the glass substrates are exempt from the possibility of lattice mismatch with molybdenum trioxide [15] besides the thickness of prepared trilayer structures is low, the amorphous nature seems to be due to the incomplete formation of particles on the substrate and presence of defects. Annealing did not affect the crystal structures of prepared samples on glass substrates and the aforementioned samples remained amorphous after annealing.

3.2 AFM and EDX Studies

To investigate the surface morphology of prepared multilayer structures with different Ag thicknesses and to study the role of thermal annealing on surface roughness of the films, atomic force microscopy (AFM) analysis with a scanning size of $5\times5\mu m^2$ has been used. The 2D and 3D AFM images of deposited samples on glass substrates at different Ag thicknesses are shown in Fig. 2.

In all these samples a uniform granular appearance is observed, so that the grain size in samples with Ag thickness of 10 nm is smaller and the grain distribution is more uniform compared to other samples. The 2D and 3D AFM images of deposited samples on glass substrates with Ag thickness of 10 nm after annealing at temperature of 400 and 500 ◦C are shown in Fig. 3. It is observed that thermal annealing has significantly affected the surface morphology of the samples, nevertheless did not affect the crystallinity of samples. After annealing and with increasing the annealing temperature, the grain size has increased. Fig. 4.(a) shows the average roughness and root mean square roughness of MAM trilayer structures deposited at different Ag thickness on glass substrates. Studies on the roughness of the multilayer structures show that the average roughness and root mean square (rms) roughness in all these samples have similar trends. In the as-deposited samples, first with increasing the Ag midlayer thickness up to 10nm, the roughness values decreased then with further enhancement in Ag thickness, increased. The average roughness and rms roughness of MA(10nm)M multilayer deposited after annealing at temperature of 400 and 500 ◦C are shown in Fig. 4(b). Studies show that annealing has led to an increase in the roughness of the samples surface. Also, the roughness values have increased with increasing the annealing temperature up to 500◦C. These changes are attributed to an increase in

grain size and change in morphology of the deposited layers. Energy- dispersive X-ray (EDX) analysis has been used to identify the elements present in samples. This technique determines the elemental details of the samples surface elements. The EDX spectra of samples deposited on glass substrates with Ag thickness of 10nm, as well as samples annealed at 400 ◦C, are shown in Fig. 5. The EDX spectra in all samples confirms the presence of oxygen, molybdenum and Ag elements and shows that the layers completely follow the composition of the target materials and are free from any contamination, which indicates the high quality of MAM prepared trilayer [18].

3.3. Optical and Electrical Properties

The optical transmittance of MAM trilayer has been investigated by ultraviolet-visible (UV-VIS) spectrometer in the wavelength range of 350-1000 nm. The optical transmittance spectra of the trilayer structures deposited on glass substrates at different Ag thicknesses and different annealing temperature are shown in Fig. 6.(a) and Fig. 6.(b). According to optical investigations the transmittance in as-deposited samples is relatively low. In general, the low transmittance in these samples is attributed to the presence of oxygen vacancies.

The lowest optical transmittance value belongs to the sample prepared with an Ag thickness of 5 nm. The transmittance value increases with increasing the Ag thickness up to 15 nm and then decreases with further increasing of Ag thickness. It is observed that with increasing the Ag thickness the transmittance peak shifts toward red wavelength. The highest optical transmittance at 550 nm corresponds to the layers deposited with intermediate Ag thicknesses of 10 and 15nm. In fact, the high difference between the refractive index of the Ag layer and the dielectric layer leads to effective Plasmon coupling, which results in desired visible transparency.

Therefore, the better transmittance at intermediate Ag thicknesses can be attributed to the surface Plasmon resonance of the Ag layer, which has been reported previously [9]. The decrease in transmittance at Ag thickness of 20 nm is caused by the increase of charge carrier densities with increasing Ag thickness, which can lead to increased absorption and decreased transmittance. By exposing the samples deposited on glass substrates at Ag thickness of 10 nm to thermal treatment at 400 ◦C in presence of oxygen gas, the optical transmittance improves. This increase can be due to the reduction of oxygen vacancies and transition to more stoichiometric molybdenum trioxide layers [10].

Thermal annealing also leads to shifting the absorption edge of molybdenum trioxide layers towards the lower wavelengths [19].

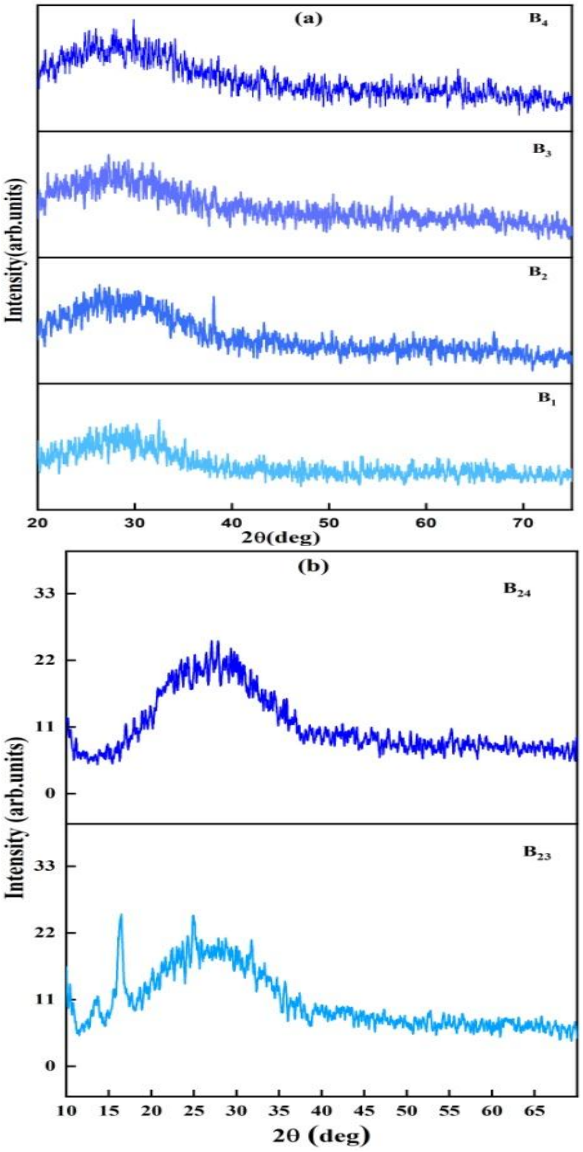

Fig. 1. XRD patterns of MoO_3/Ag/MoO_3 trilayer films: (a) at different Ag thickness and (b) after annealing at 400 ◦C (B_{23}) and 500 ◦C (B_{24}).

Oxygen vacancies can create further electronic states in the energy gap of MoO_3 and form a narrow donor band below the conduction band. Reducing oxygen vacancies by thermal annealing, decreases the number of these excess states and increases the optical band gap, shifting the absorption edge to lower wavelengths [10, 20]. With increasing the annealing temperature to 500 ◦C, the optical transmittance decreases significantly. Morphological studies showed that annealing at this temperature resulted in a high surface roughness of the samples, so the sudden drop in transmittance could be due to increased absorption and scattering caused by the high surface roughness. The sheet resistance of MAM trilayer structures deposited on glass substrates at different Ag thickness and after annealing at temperature of 400 and 500 ◦C at an Ag thickness of 10 nm has been investigated using the

four-point probe technique. The numerical results of the measurements are summarized in Table 2. It is observed that the electrical conductivity of layers clearly depends on the thickness of Ag layer. With increasing Ag thickness, the sheet resistance values decrease, while at Ag thickness of 10 nm there is a sudden decrease. This decrease is explained by the formation of threshold percolation pattern and transition from a discontinuous Ag layer to a continuous layer [7]. When the Ag thickness in trilayer structures increased to 10 nm, their sheet resistance values decrease significantly, so there is a possibility of Ag islands existence at the Ag layer thickness of 5 nm [10], which is in agreement with the decrease in samples roughness values after changing the thickness of Ag layer to 10 nm and also in agreement with the results of study [21] in which the roughness values increased due to island growth. Island boundaries can act as disconnected scattering sites and reduce the mobility of charge carriers and the reduction in mobility of charge carriers leads to a decrease in their density and consequently, to a higher sheet resistance [10]. By changing the Ag thickness layer to 10 nm, the discontinuous Ag layers were replaced by continuous and uniform layers, which resulted in lower sheet resistance in this sample. Thermal annealing has led to improved electrical conductivity. Since annealing was performed in the presence of oxygen gas and there is no possibility of reducing oxide state in MoO_3 layers, Improvement in conductivity through thermal annealing can result from increasing the density of the MoO_3 layers or from structural ordering within the layers. Sometimes, the layers may become slightly more compact after annealing without the appearance of any distinct diffraction peaks. Island boundaries can act as disconnected scattering sites and reduce the mobility of charge carriers and the reduction in mobility of charge carriers leads to a decrease in their density and consequently, to a higher sheet resistance [10]. By changing the Ag thickness layer to 10 nm, the discontinuous Ag layers were replaced by continuous and uniform layers, which resulted in lower sheet resistance in this sample. Thermal annealing has led to improved electrical conductivity. Since annealing was performed in the presence of oxygen gas and there is no possibility of reducing oxide state in MoO_3 layers, Improvement in conductivity through thermal annealing can result from increasing the density of the MoO_3 layers or from structural ordering within the layers. In this research, multilayer structures of MoO_3/Ag/MoO_3 with good electrical and optical properties for use as TCE have been designed.

A figure of merit is a numerical value used to evaluate and compare the performance of different devices, systems or methods based on their key parameters.

It indicates how well the devices, systems or materials perform relative to their alternative in a particular application. To investigate the performance of transparent conductive multilayer prepared on glass substrates, we have used the figure of merit defined by Hock [22] Eq. 1.:

$$\mathrm{FOM} = \frac{T^{10}}{R_S} \qquad \text{Eq. (1).}$$

FOM indicates the figure of merit, T is optical transmittance and R_S represents the sheet resistance. We have calculated the figure of merit at 550 nm for the MoO_3/Ag/MoO_3 trilayer structures deposited on glass substrates. The calculation results are given in Table. 3. The highest figure of merit value was obtained at Ag thickness of 15 nm and then at Ag thickness of 10 nm. However, achieving high performance TCEs requires high optical transparency and electrical conductivity and also an appropriate surface roughness.

Therefore, a compromise optimization must be made between the optical transmittance, electrical conductivity and surface roughness of prepared samples.

For this purpose we chose the MA (10nm) M as the ideal sample and performed thermal annealing on this structure. After annealing at temperatures 400 and 500 ◦C, the figure of merit values first increased significantly and then decreased. Therefore, the optimal structure is the glass/MoO_3/Ag (10nm)/MoO_3 which annealed at 400 ◦C. Fig. 7.(a) and Fig. (b). show the variation of the FOM and sheet resistance value with Ag thickness and annealing temperature. It is observed that thermal annealing plays a prominent role in modifying the electrical and optical properties and consequently the figure of merit of the MAM structures. Annealing at temperature of 400 ◦C leads to a decrease in sheet resistance and an increase in optical transmittance of MAM structures compared to the pristine samples, indicating a trade-off between transparency and electrical conductivity at this temperature, and demonstrating the importance of annealing in achieving the best performance.

The optimal structure, with a superior figure of merit of 23.86×10^{-3} (Ω^{-1}) is suitable candidate as transparent conductive electrodes in optoelectronic devices and solar cells. It can be concluded that thermal annealing is an efficient method in improving the optical transmittance, electrical conductivity and consequently performance of prepared multilayer structures as transparent electrodes.

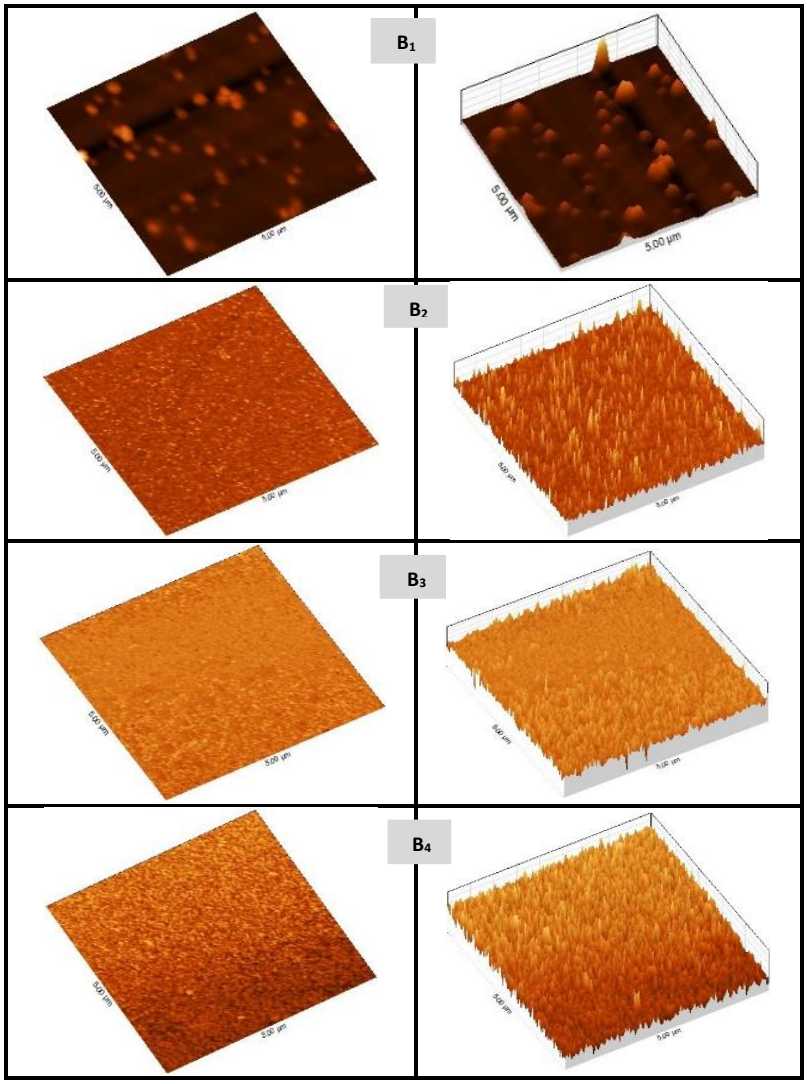

Fig. 2. 2D and 3D images of the MoO_3/Ag/MoO_3 trilayer films at different Ag thicknesses.

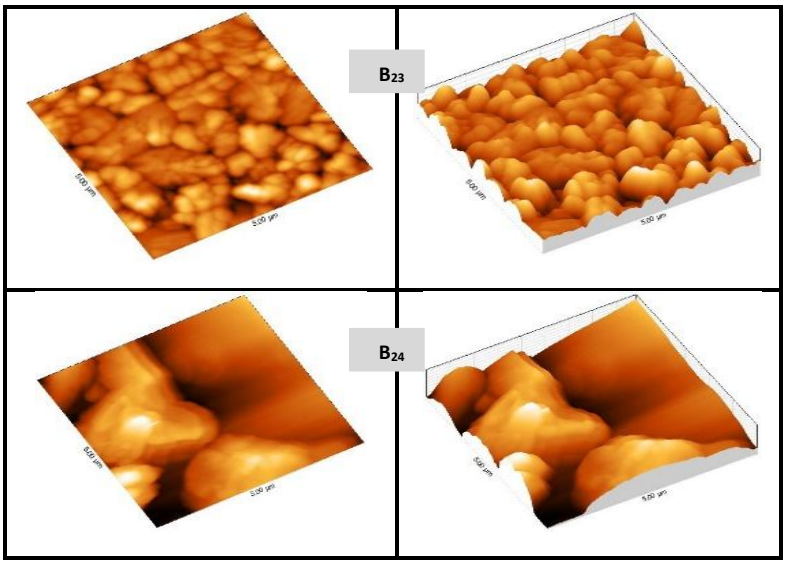

Fig. 3. 2D and 3D images of the MoO_3/Ag/MoO_3 trilayer films at Ag thickness of 10 nm: annealed at 400 ˚C (B_{23}) and 500 ˚C (B_{24}).

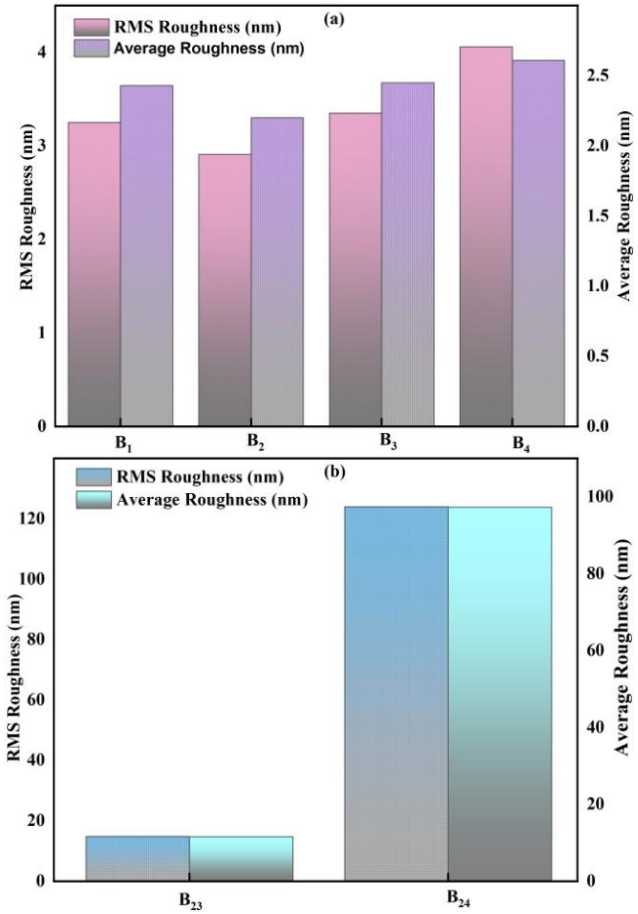

Fig. 4. The root mean square (Rms) and average roughness of $MoO_3/Ag/MoO_3$ trilayer films: a) at different Ag thickness b) at Ag thickness of 10 nm and annealed at 400 °C (B_{23}) and 500 °C (B_{24}).

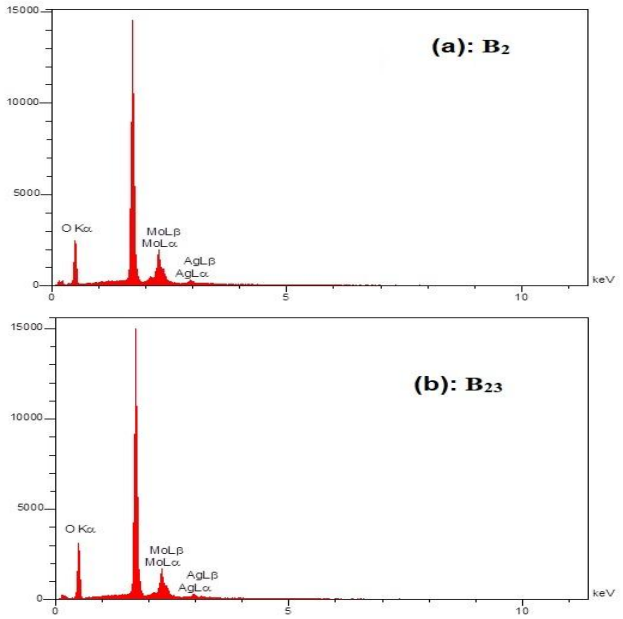

Fig. 5. EDX spectra of (a) the as-deposited sample B_2 and (b) annealed sample B_{23} at temperatures of 400 °C.

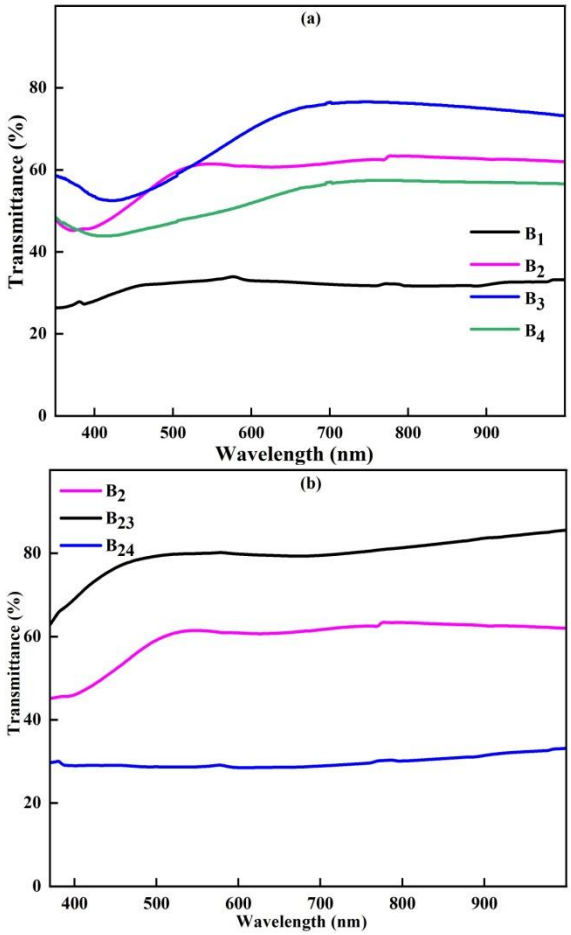

Fig. 6. Transmittance spectra of $MoO_3/Ag/MoO_3$ trilayer films deposited on glass substrate: a) as-deposited samples at different Ag thicknesses b) annealed samples at temperatures 400°C (B_{23}) and 500 °C (B_{24}).

Table. 2. The Sheet Resistance of the as-deposited and annealed $MoO_3/Ag/MoO_3$ trilayer films.

Sample	Ag Thickness (nm)	Annealing Temperature (k)	Sheet Resistance (Ω/sq)
B_1	5	-	11.8
B_2	10	-	9.1
B_3	15	-	7.2
B_4	20	-	5.7
B_{23}	10	400	4.5
B_{24}	10	500	5.1

Table. 3. The optical and electrical parameters of the as-deposited and annealed MoO_3/Ag/MoO_3 trilayer films.

Sample	Ag Thickness (nm)	Annealing Temperature (°C)	Transmittance (λ=550 nm) (%)	Sheet Resistance (Ω/sq)	Figure of Merit 10^{-3} (Ω^{-1})
B_1	5	-	33.15	11.8	0.001
B_2	10	-	61.45	9.1	0.90
B_3	15	-	64/0	7.2	1.60
B_4	20	-	49.30	5.7	0.15
B_{23}	10	400	80.0	4.5	23.86
B_{24}	10	500	28.71	5.1	0.008

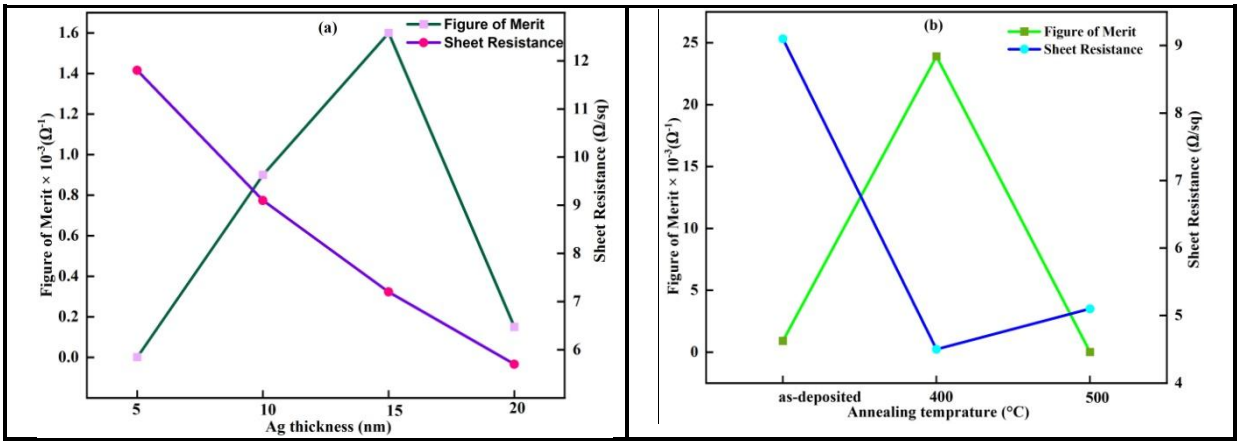

Fig. 7. The variation of figure of merit and sheet resistance values of MoO_3/Ag/MoO_3 trilayer films as a function of (a) Ag thickness and (b) annealing temperature.

4. Conclusion

1. Symmetric MoO_3/Ag (5, 10, 15, 20 nm)/ MoO_3 structures deposited on glass substrates using RF and DC magnetron sputtering.
2. Amorphous uniform and granular appearance with low optical transmittance observed.
3. Electrical conductivity enhanced by increasing the Ag thickness.
4. Creation of threshold percolation pattern and transition from a discontinuous Ag layer to a continuous one formed at Ag thickness of 10 nm.
5. MA (10nm) M with better features was reactively annealed at 400 and 500 °C.
6- Surface roughness increased in all samples.
7. At 400 °C, sheet resistance values decreased and transmittance improved in glass/MAM samples.
8. Absorption edge of molybdenum trioxide layers shifted towards the lower wavelengths after annealing.
9. Glass/M/A(10nm, 400 °C)/M with figure of merit of 23.86×10^{-3} (Ω^{-1}) ideal as TCE in optoelectronic devices like solar cells.

References

[1] Al-Kuhaili MN, Transparent-conductive and infrared-shielding WoO_3/Ag/WoO_3 multilayer heterostructures. Solar Energy. 2023; 250:209–219.
[2] Kao PC, Hsieh CJ, Chen ZH, Chen SH, Improvement of MoO_3/Ag/MoO_3 multilayer transparent electrodes for organic solar cells by using UV-ozone treated MoO_3 layer. Solar Energy Materials and Solar Cells. 2018; 186:131–141.
[3] Su M, Shi S, Chen J, Ren D, Yue L, Meng F, Preparation and optimization of MTO/Ag/MTO transparent flexible film based on co-sputtering at room temperature. Applied Physics A. 2024; 130:406.
[4] Chang L, Daun L, Sheng M, Yuan J, Yi H, Zou Y, Uddin A, Optimizing non-patterned MoO_3/Ag/MoO_3 anode for high performance organic solar cells towards window applications. Nanomaterials. 2020; 10:1759.
[5] Park JY, Kim HK, Flexible Metal/Oxide/Metal transparent electrodes made of thermally evaporated MoO_3/Ag/MoO_3 for thin film heaters. Physica Status Solidi A. 2018;215(23).
[6] AnnabiMiilani E, Piralaee M, Raeyani D, Asgari A, High-performance semi-transparent organic solar cells for window applications using MoO_3/Ag/MoO_3 transparent anodes. Solar Energy Materials and Solar Cells. 2024;276(11):113066.
[7] Cattin L, Lare Y, Makha M, Fleury M, Chandezon F, Abachi T, Morsli M, Napo K, Addou M, Bernede JC, Effect of the Ag deposition rate on the properties of conductive transparent MoO_3/Ag/MoO_3multilayer. Solar Energy Materials and Solar Cells. 2013; 117:103–109.
[8] Xu TN, Hu L, Jin SQ, Zhang BP, Cai XK, Wu HZ, Sui CH, Photon energy conversion via localized surface plasmons in ZnO/Ag/ZnO nanostructures. Applied Surface Science. 2012;258(15):5886–5891.

[9] Cattin L, Morsli M, Dahou F, Yapi Abe S, Khelil A, Bernede JC, Investigation of low resistance MoO_3/Ag/MoO_3 multilayer and application as anode in organic solar cells. Thin Solid Films. 2010; 518:4560–4563.
[10] Kaoa PC, Hsua CJ, Chena ZH, Chena SH, Highly transparent and conductive MoO_3/Ag/MoO_3 multilayer films via air annealing of the MoO_3 layer for ITO-free organic solar cells. Journal of Alloys and Compounds. 2022; 906:164338.
[11] Rani S, Kumar A, Ghosh DS, Effect of rate of deposition on opto-electrical characteristics of vapor deposited MoO_3/Ag/MoO_3 transparent electrode for photovoltaic applications. Materials Today: Proceedings. 2023.
[12] Park W, Kumar M, Kim J, Chung Y, Park H, Catalyst free single-step processes to grow crystalline MoO_3 nanowires by reactive sputtering method. Materials Science in Semiconductor Processing. 2018; 79:40–45.
[13] Cattin L, Louarn G, Morsli M, Bernede JC, Semi-transparent organic photovoltaic cells with dielectric/metal/dielectric top electrode: influence of the metal on their performances. Nanomaterials. 2021;11(2).
[14] Lee CY, Chen YM, Deng YZ, Kuo YP, Chen PY, Tsai L, Lin MY, Yb: MoO_3/Ag/MoO_3 multilayer transparent top cathode for top-emitting green quantum dot light emitting diodes. Nanomaterials. 2020; 10:663.
[15] Raza SH, Afzal N, Rafique M, Imran M, Ahmad R, Structural and morphological properties of annealed MoO_3 films on different substrates. Surface Review and Letters. 2019;27(5):1–12.
[16] Sivakumar R, Jayachandran M, Sanjeeviraja C, Effect of annealing on structural, surface and optical properties of PVD-EBE α-MoO_3 thin films for electrochromic devices. Surface Engineering. 2004;20(5):385–390.
[17] Hojabri A, Hajakbari M, Emami Meibodi, Moghri Moazzen M, Influence of thermal annealing oxidation temperature on the structural and morphological properties of MoO_3 thin films. Acta Physica polonica A. 2013;123(2):307–308.
[18] Feyzi E, Hajakbari M, Hojabri A, Influence of annealing temperature on the structural, morphological, and optical properties of nanocrystalline NiO thin films and its application in acetone gas sensing. Journal of material science:Material in electronics 2023;34(11):971.
[19] Hojabri A, Adavi M, Hajakbari F, Synthesis of nickel-doped TiO_2 thin films and their structural and optical properties at different annealing temperatures. Acta Physic Polonica A,2017,131(3),386-388
[20] Mandal B, Aaryashree A, Das M, Than Htayb M, Mukherjee S, Architecture tailoring of MoO_3 nanostructures for superior ethanol sensing performance. Materials Research Bulletin. 2019; 109:281–290.
[21] Zadsar M, Fallah HR, Haji Mahmoodzadeh M, Tabatabaei SV, The effect of Ag layer thickness on the properties of WO_3/Ag/MoO_3 multilayer films as anode in organic light emitting diodes. Journal of Luminescence. 2012;132(4):992–997.
[22] Nouri Z, Hajakbari F, Hojabri A, Impact of annealing temperature on physical properties of transparent conductive MoO_3/Ag/MoO_3trilayer films grown by sputtering. Applied Physics A. 2025; 131:282.